INFLUENCE OF ABUTMENT RESTRAINTS ON THE SEISMIC RESPONSE OF MULTI-SPAN CONTINUOUS BRIDGES

A. Dall'Asta[1], E. Tubaldi[2] and L. Ragni[2]

[1] *Department PROCAM, University of Camerino, Ascoli Piceno, Italy*
[2] *DACS, Marche Polytechnic University, Ancona, Italy*
Email: andrea.dallasta@unicam.it

ABSTRACT :

The performance of multi-span steel-concrete composite bridges in recent seismic events has shown that these structures are very sensitive to earthquake loading. Extensive damage may occur not only in the substructures, which are expected to yield, but also in the components of the superstructure involved in transferring the seismic loads. Current codes allow the design of regular bridges by means of linear analysis based on response spectrum reduced by a reduction factor reflecting their structural ductility capacity. In bridges whose superstructure transverse motion is restrained at the abutments the sequential yielding of the piers may cause a substantial change of the stiffness distribution. As a consequence force distribution and displacement demand may notably differ from the predictions provided by linear analysis.
The scope of this paper is to assess the influence of piers-deck stiffness ratio and piers-deck strength ratio in the post elastic seismic behavior of continuous composite bridges. Some results concerning a three span continuous slab on girder bridge are presented. The dependence of the response on these parameters is studied by means of incremental nonlinear dynamic analysis. The results are then compared with those obtained by means of a linear dynamic analysis. Main focus is posed on curvature demand of the piers, bending moments acting on the superstructures and reaction forces in correspondence of the piers and the abutments.

KEYWORDS: Composite bridges, transverse seismic behavior, reduction factor

1. INTRODUCTION

Recent seismic events all over the world have shown that bridge structures are particularly sensitive to earthquake loading. One of the current practices for earthquake resistance design of bridges involves the formation of plastic hinges at the base of piers during severe shaking in order to bring down the seismic design forces to acceptable levels. Other members such as deck, bearing devices, abutments and foundations must be designed to remain elastic in order to avoid brittle failure. The performance of multi-span steel-concrete composite bridges in recent earthquakes has shown that extensive damage can occur not only in the substructures, which are expected to yield, but also in the components of the superstructure involved in transferring the seismic loads (Itani et al. (2004)). A correct evaluation of the real forces and of the displacement demands for every structural element of the bridge involved in the seismic loads path is therefore crucial.
In many cases a transverse constraint is introduced at the abutments in order to reduce deck bending and to avoid expensive bi-directional joints. In this situation the sequential yielding of the piers may cause a substantial change with respect to the force and displacement distributions predicted by Response Spectrum Analysis (RSA). These bridge configurations are commonly referred as "Bridges with Dual (Elastic and Inelastic) load paths" in Calvi (2004). In fact, only a portion of the inertia forces developed in the deck is transmitted to the pier footings by column bending while the remainder is transmitted to the abutments by superstructure bending. The transfer mechanism involving the piers is referred as the inelastic path because piers are expected to yield in order to dissipate energy, while the second mechanism involving the deck and the abutments is the elastic path because structural components are supposed to remain elastic. For low values of the seismic intensity the portion of load carried by each path strongly depends on the relative effective column and deck stiffness as well as on the degree of lateral restraint provided at the abutments. It is however evident that for growing values of the seismic intensity piers yield and the additional seismic demand must completely be absorbed by the superstructure. Consequently, abutments reactions and superstructure bending moments continue to grow.
Despite of such complex post-elastic behavior, linear analysis based on response spectrum reduced by the

reduction factor is nowadays the most popular method used to predict the behavior of regular bridges subjected to transverse input motion.
The major part of the studies about transverse behavior of continuous bridges under seismic loading are focused on the limit of results which can be deduced from linear analysis based on response spectra (Benzoni et al. (2003), Fardis et al. (2007), Calvi (2004), Priestley (2007)) while few studies investigate the consequences of limited strength and deformability of the deck on the global behavior and the relevant modeling problems (Panagiotakos et al. (2006), Itani et al. (2004), Fardis et al. (2007)).
The present study aims at assessing the main parameters that affect the transverse dynamic behavior of continuous slab on steel girder regular bridges, widely used in Europe in the range of short and medium spans due to their high performance and simplicity. If the flexibility of the abutment restraints due to end cross-diaphragm deformability and to soil-structure interaction is neglected, then piers stiffness, deck stiffness and their ratio are the only parameters that can significantly influence the transverse seismic behavior of these bridges. A parametric analysis is performed for different values of the piers height, maintaining unvaried the deck and the column transverse section, considering a study case consisting of a three span continuous bridge. The dependence of the response on these parameters is studied by means of Incremental Dynamic Analysis (IDA). Main focus is posed on curvature demand of the piers and the deck, bending moments distribution in the superstructures and reaction forces in correspondence of the piers and the abutments at ultimate condition. Furthermore, results obtained with nonlinear analyses are compared with those obtained by means of linear analyses in order to evaluate the limits of an analysis based on the reduction factor.

2. STUDY CASE AND PARAMETRIC ANALYSIS

The bridges analyzed in this paper have a total length of 130 *m* divided into 3 spans respectively 40, 50 and 40 *m* long (Fig.1). The superstructure consists of a 12 *m* large slab which can host 2 lanes and of two steel girders 6 *m* spaced. The distributed weight, including asphalt and super-dead loads, is taken as 138 *kN/m*. Deck slab is haunched and the thickness varies between 200 *mm* and 350 *mm*. The deck is transversally fixed at the abutments.
The support to the deck is provided by two reinforced concrete piers with a circular section of diameter D=2.2*m*. In the parametric analysis the piers aspect ratio H/D between columns height H and cross section diameter D is varied from 3.0 to 9.0 (H spans from 6.6 *m* to 19.8 *m*). In this way the it is possible to investigate the influence of the pier stiffness and pier resisting forces on the global bridge response. Smaller heights are not considered because the aspect ratio H/D would result too small and the shear behavior prevails on flexural deformation. Piers higher than 20 *m* are also not considered because an hollow section is usually preferred in these situations in order to reduce the pier mass. The circular columns have a fixed longitudinal reinforcement ratio equal to 1% of the concrete area. Transverse reinforcement with a volumetric ratio ρ_w of about 0.5% has been provided in the hinge region with the aim of confining concrete and preventing premature shear failure, whatever is the column height adopted.

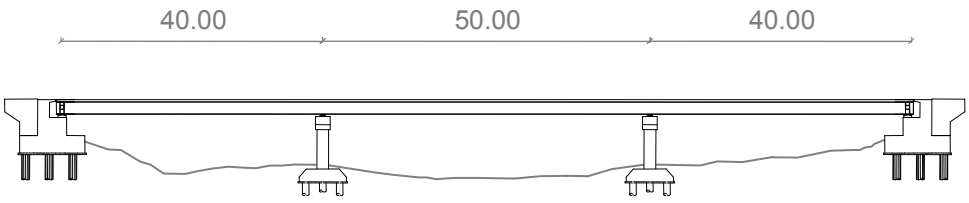

PIERS	
Concrete:	C30/37
Steel (reinforcement):	B450C

DECK	
Concrete:	C35/45
Steel (girders):	S355
Steel (reinforcement):	B450C

Figure 1 Bridge longitudinal profile and basic properties of materials

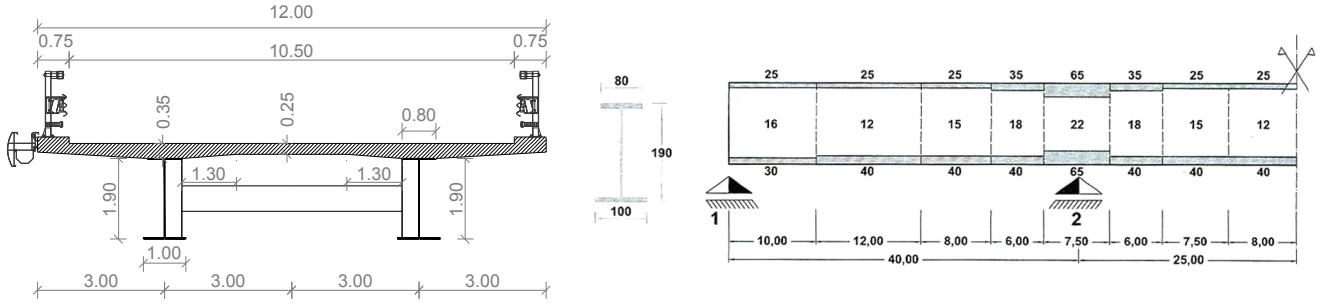

Figure 2 Deck transverse section and cross section distribution

3. STRUCTURAL ANALYSIS

In the analysis of the superstructure under the seismic load combination, the effects of the vertical permanent loads must be combined together with the effects induced by earthquake action. This aspect assumes a particular relevance in composite bridge where the concrete slab cracking influences the section stiffness. In correspondence of the piers (hogging regions) permanent actions induce negative moments which result in traction effect on the concrete slab and compression in the steel girders. Conversely, in the sagging regions bending moments are reverted and concrete deck is compressed. For this reason different amounts of longitudinal reinforcement are provided along the deck, 2% of the slab area above the supports, 1% at midspan. The stress induced by concrete creep and shrinkage is neglected.

The deck capacity is evaluated according to EC8-part 2 where values of strain limits under seismic action are suggested. The girder cross section varies along the bridge and consequently its yielding moment under transverse deformation $M_{y,d}$ is not constant. Minor variation can also be observed in the values of the yielding curvature $\phi_{y,d}$. This parameter is mainly influenced by the deck width and material yield strains which remain constant along the bridge.

The superstructure is described by three-dimensional frame elements. A fiber mode is adopted in order to describe the cracking concerning vertical bending due to gravitational loads and non-linear behavior related to transverse bending due to seismic loads. Slab concrete behavior is provided by Kent-Scott-Park Model (Kent and Park (1971)). Degraded linear unloading/reloading stiffness is taken into account according to Karsan-Jirsa (Karsan and Jirsa (1969)) and tensile strength is neglected. Reinforcement steel is modeled by an elasto-plastic material with a yield stress $f_{ym} = 517 N/mm^2$, an elastic modulus $E_s = 210000 N/mm^2$, a strain hardening ratio $b = 0.0008$ and a ultimate strain $\varepsilon_{su} = 0.075$. Girders' steel remains within the elastic range in the performed analysis and thus only the elastic modulus is assigned.

Piers are represented by three-dimensional frame elements which pass through the geometrical centre of the columns and the cap beam. A rigid end zone (1.81 m in length) is located at the top of the columns in order to account for the offset between the center line of the cap beam and the center line of the deck. A lumped plasticity model is adopted to reproduce the inelastic behavior expected at the base of the column in the plastic hinge zone. Plastic deformations are assumed to be concentrated along the length L_p, expressed in EC8- part 2 as:

$$L_p = 0{,}10 \cdot L + 0{,}015 f_{yk} \cdot d_s \qquad (3.1)$$

being f_{yk} and d_s respectively the characteristic yield stress and the diameter of reinforcements, while L is the distance from the plastic hinge to the section of zero moment.

A "Beam with Hinges" element (Scott and Fenves (2006)) is used to model the columns. This element is based on flexibility formulation and assumes plasticity spreading over specified hinge lengths L_p at the element ends. The effect of confinement on the concrete core in the plastic hinge zone is taken into account according to Appendix E of EC8-part 2 : concrete compressive strength is found to increase from the value of $38 N/mm^2$ to

$45.9 N/mm^2$ while the ultimate deformation increases from the value of 0.0035 to 0.00968.
Outside the plastic hinge length, pier and cap elements with an elastic section are introduced. Their effective stiffness EI_{eff} is determined according to the procedure defined in EC8-part 2, on the base of the ultimate moment M_u and yielding curvature ϕ_y:

$$EI_{eff} = 1.2\frac{M_u}{\phi_y} \tag{3.2}$$

Incremental dynamic analyses (Vamvatsikos (2002)) are performed by using three independent input ground motions generated so as to match the target EC8-Type 1 Response Spectrum for 5% viscous damping. The PGA of the site on which the bridge stands is 0.3g (ag = 0.25g, Type B Subsoil). The amplitudes of the ground accelerations are uniformly scaled up by a scalar $\lambda \in [0,+\infty)$ in order to cover the whole range of structural behavior up to failure. The viscous damping in nonlinear analysis is evaluated at each step using the tangent stiffness matrix (Priestley et al. (2007)). Ultimate conditions are considered to be met either when piers have reached their ultimate curvature or when the deck has yielded. Piers and abutments reactions, deck bending moments, displacement of the center of the mass of the superstructure are recorded as a function of λ. The reported results refer to the average values obtained from the three input ground motions.
Non-linear results are then compared with that obtained performing linear time history analysis (LTHA) for the same scaled ground accelerations. In the linear model elastic beam elements are adopted for deck and piers by considering the effective stiffness values EI_{eff} resulting from moment-curvature diagrams.
Structural analyses have been performed with the support of the finite element software Opensees (McKenna, F., et al. (2006)).

4. RESULTS

The eigenvalue analysis has provided the periods and the elastic modal shapes for the different ratios *H/D*. The calculated modal periods *T* and mass participation factors *MPF* are summarized in Figure 3 (only transverse direction is considered). Participating mass of the first period slightly varies for increasing values of *H/D*. The second and the third transverse modes play a very little role in the bridge response.

H/D	*T(sec)*	*MPF*
3.0	0.6257	0.7909
3.5	0.731	0.7309
4.0	0.827	0.7906
5.0	0.995	0.7971
6.0	1.127	0.8029
7.0	1.228	0.7977
8.0	1.306	0.7883
9.0	1.364	0.7762

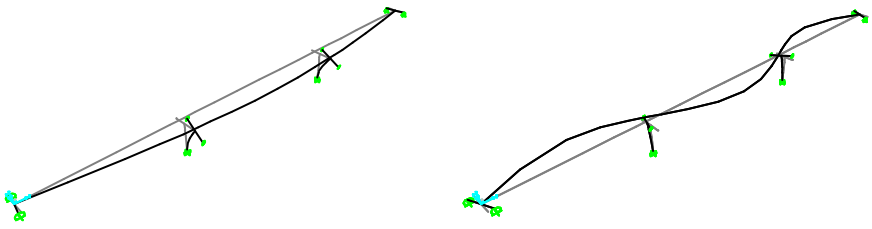

Mode 1- deformed shape *Mode 3- deformed shape*

Figure 3 Modal analysis results

Figure 4 describes the global behavior of the two extreme cases corresponding to the values *H/D*=3 (Fig. 4a) and *H/D*=9 (Fig.4b). The two graphs describe the relationship between the displacement of the center of the mass d_c and the reaction force sum of abutments and piers.
In the first case it is evident that for low intensities of the seismic action piers attract high seismic forces since they are very stiff. For values of λ close to 0.8 plastic hinges form at the base of the piers therefore their reaction forces cannot increase further. As a consequence seismic load path involving abutments becomes more and more important for higher values of λ. Piers are found to reach their ultimate displacement before the deck yields for $\lambda = 3.5$.
In the second case (*H/D*=9) piers are very flexible and they yields for $\lambda = 1.5$ while failure is attained when deck reaches its yielding curvature at midspan. The maximum value of PGA (corresponding to $\lambda = 2.35$) is

thus limited by deck yielding which occurs before of the pier failure.

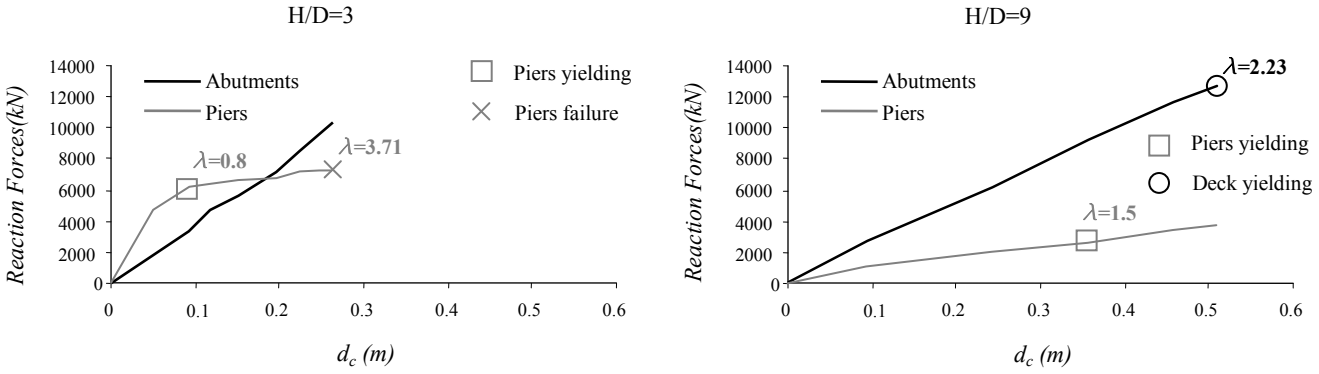

(a) (b)

Figure 4 Abutments and piers reaction forces vs control node displacement for H/D=3 (a) and H/D=3 (b)

To evidence the location of critical sections along the deck the graphs reporting the evolution of the moment diagrams are plotted in Figure 5 for increasing values of the scale factor up to failure. The "step" in the diagrams in correspondence of the piers is due to the torsional stiffness of the piers mobilized by the deck bending. From the observation of the results concerning *H/D*=3 (Figure 5a) it is possible to argue that superstructure moments at ultimate condition are lower than the yielding values of the deck. For what concerns the case *H/D*=9 (Figure 5b) it can be observed that the moment distribution is slightly influenced by the piers. At failure the maximum value of bending moment reaches the yielding values at midspan.
The variation of the shape of the diagram can be observed in the Figure 6, which compares the two distributions of the moments for $\lambda = 0.5$ (corresponding to elastic behavior) and at failure, normalized with respect to the maximum moment found in each case. In the case of short piers (a) large differences exist between the diagram shape observed in elastic range and at failure while negligible differences occur for high piers (b).

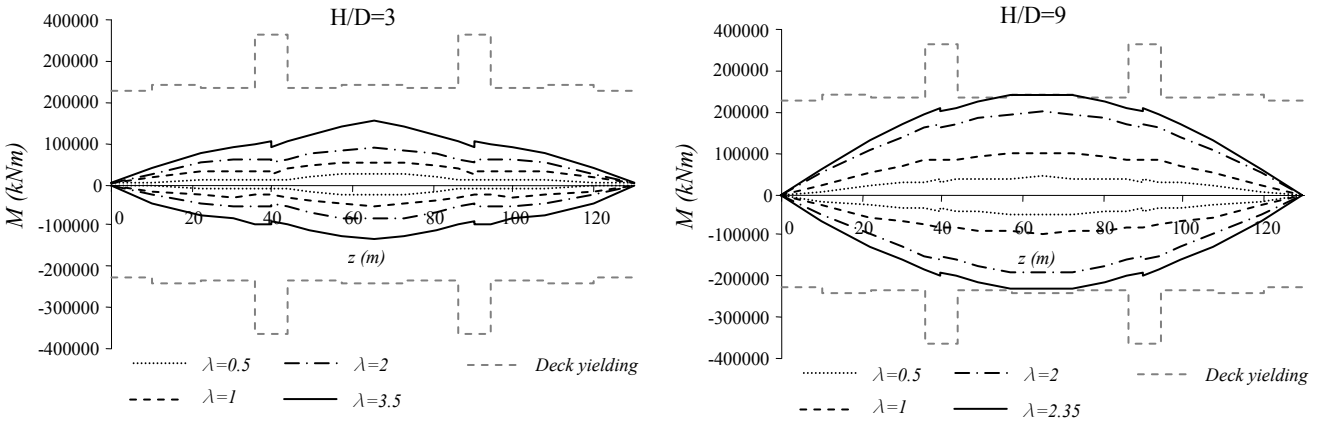

(a) *(b)*

Figure 5 Transverse bending moments for increasing values of λ for H/D=3 (a) and H/D=3 (b)

Figure 7 shows the maximum values of ground acceleration the bridge is able to withstand as a function of *H/D*: Large variation of the ultimate multiplier λ_u occurs. For short piers the ultimate value is due to piers failure and slightly increases by increasing slenderness. For larger *H/D* ratio the ultimate value is controlled by the strain limit of the deck and it decreases because the plastic pier strain and related energy dissipation are more and more reduced when pier slenderness increases. The maximum value of acceleration is attained when the piers failure occurs together with the deck yielding.

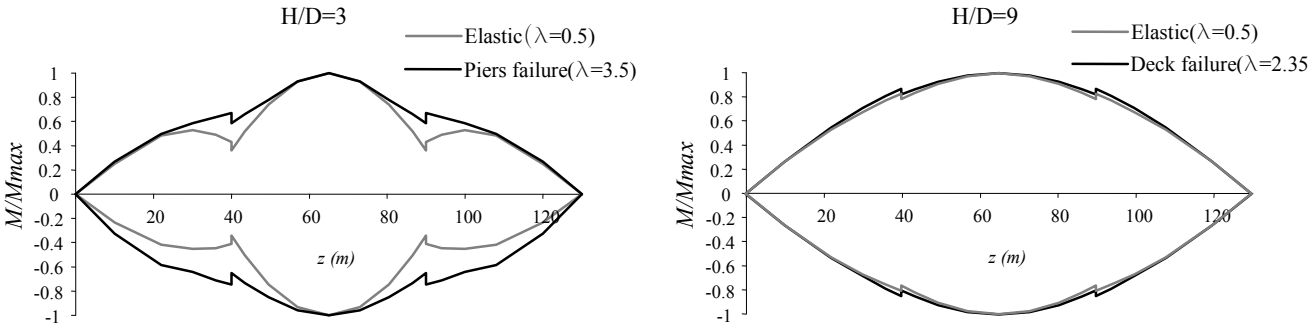

(a) *(b)*

Figure 6 Normalized transverse moment diagrams

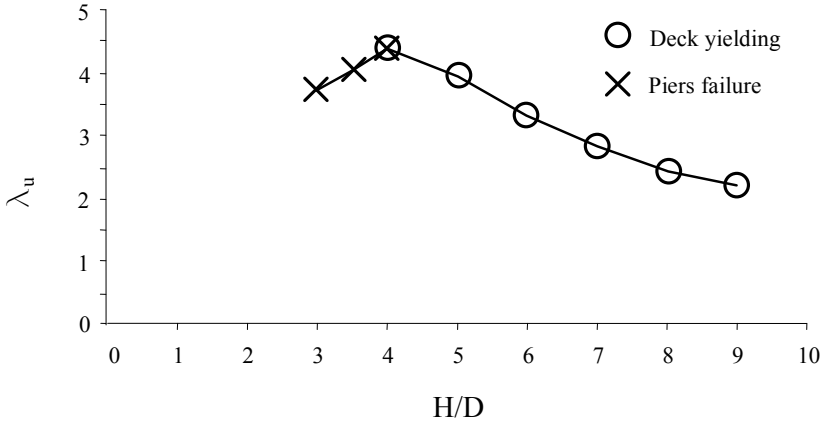

Figure 7 Multiplier λ_u versus slenderness *H/D*

Many design procedures suggested in codes of practice involve linear analyses and are based on a reduction factor defined as the ratio between the response force of the structure assumed to remain linear and the response force of the hysteretic nonlinear structure. Having in aims to evaluate the applicability of this approach to the case considered, the results of the nonlinear analysis are compared with the results furnished by linear analysis. The intermediate case *H/D*=3.5 (piers failure) is discussed in detail.

Figure 8 reports the reaction forces on the piers (a), the reaction forces at abutments (b) and the global reaction force (c) as functions of the control node displacement d_c. The control node displacement d_c versus seismic action multiplier λ is depicted in the last graph (d). Piers show an extensive inelastic behavior and maximum forces evaluated in the piers by LTHA are very different from inelastic ones, about 5.88 times higher. This value doesn't correspond however to the ductility of the piers (about 3.74) because the maximum displacement is different in the two analyses. Lower differences can be observed in the abutment reaction forces and similar results have been obtained for all the seismic levels considered. Finally, the last two graphs take in evidence that displacements predicted by NTHA in the non-linear range are lower than displacements predicted by LTHA. The equal displacement rule, which holds for SDOF elasto-plastic systems, seems to not apply in this case.

In Figure 9 the ratio between linear and non-linear response at the ultimate condition for different values of the slenderness *H/D* is reported. More precisely, the four graphs of Figure 9 refer to the ratios concerning the following quantities: pier forces (a), abutment forces (b), deck bending moments (c) and the control node displacement (d). The reduction factor of pier forces strongly reduces for high piers in consequence of the displacement limitation induced by deck strain limit. It starts from large values and approaches values close to one for *H/D*=9. A different situation occurs for abutments and values close to one are obtained for different piers slenderness. Minor variations are observed for deck bending moments at intermediate supports and at midspan. A similar situation is obtained for the control node displacement.

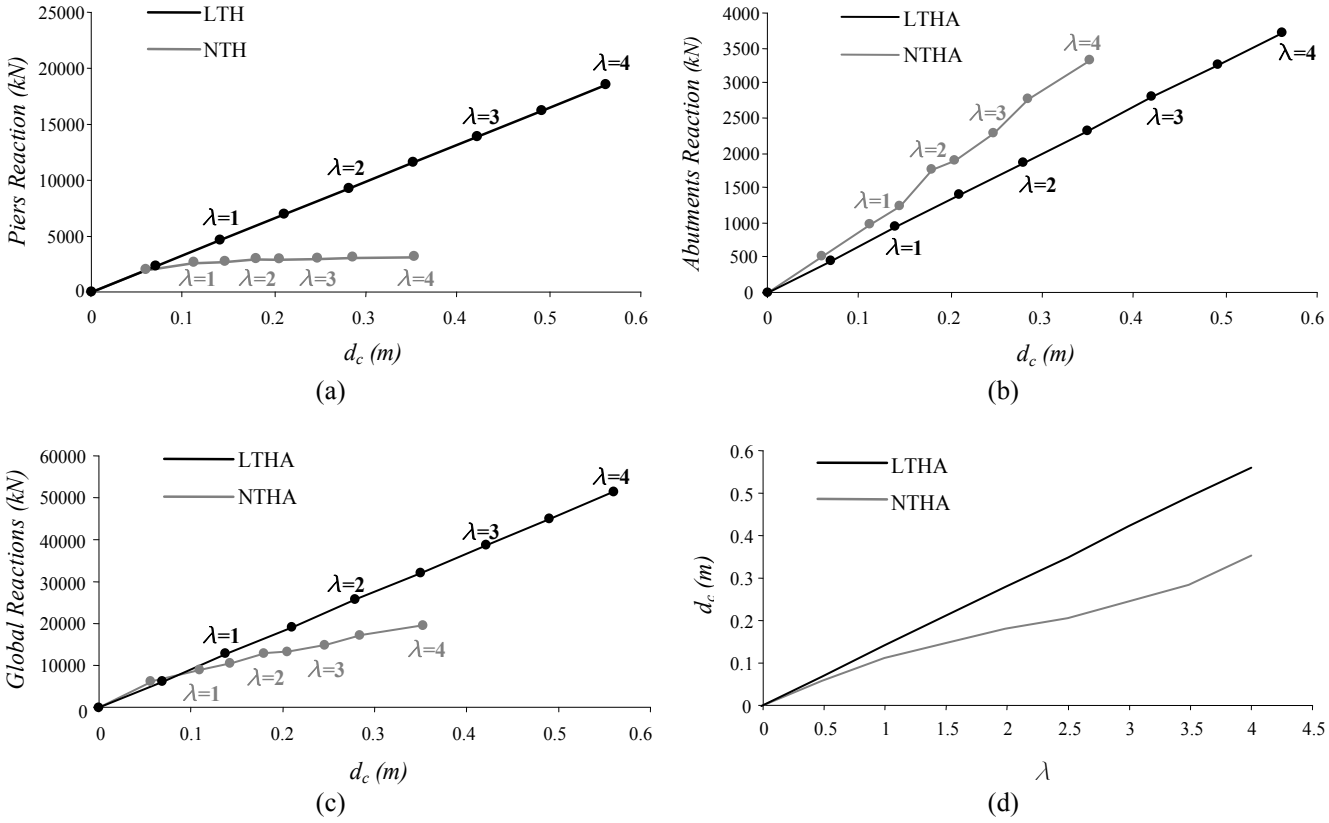

Figure 8 Linear versus nonlinear results

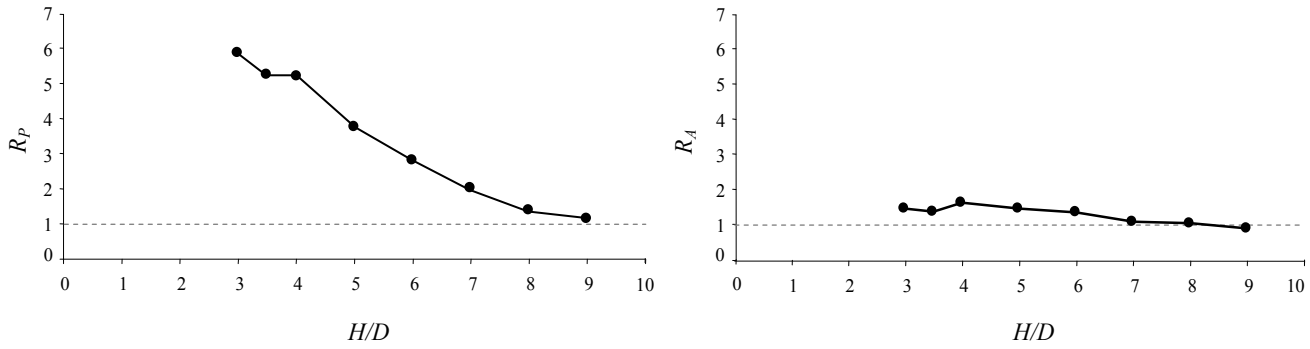

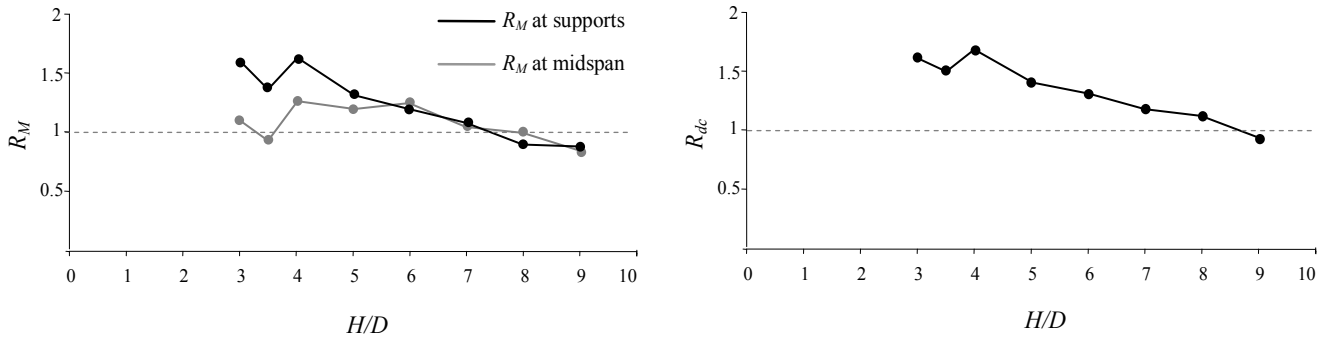

Figure 9 Elastic/inelastic result ratios

REFERENCES

Benzoni, G., Limongelli, M.P., Priestley, M.J.N. (2003). Assessment of Shear Forces on Bridge Abutments: Simplified Method, *Journal of Bridge Engineering ASCE* **8:1**, 29:38.

Calvi G.M. (2004). Recent experience and innovative approaches in design and assessment of bridges. *Proceedings of 13th World Conference on Earthquake Engineering*, Vancouver, B.C., Canada. August 1-6, 2004 Paper No. 5009.

European Committee for Standardization (2005), Eurocode 8- Design of structures for earthquake resistance – Part 2: Bridges, EN1998-2, Brussels.

Dipartimento Protezione Civile (2005), Norme tecniche per il progetto sismico dei ponti, OPCM 3431-Allegato 3 (in italian).

Fardis, M. N. and Pinto , P. E. (2007). Guidelines for displacement-based design of building and bridges, LESSLOSS Report No. 2007/05, IUSS Press, Pavia, Italy.

Itani, A.M., Bruneau, M., Carden, L., Buckle, I.G. (2004). Seismic Behavior of Steel Girder Bridge Superstructures *Journal of Bridge Engineering*, **9:3**, 243:249

Karsan, I.D. and Jirsa, J.O. (1969). Behavior of concrete under compressive loading, *Journal of the Structural Division* **95:12**, 2543-2563.

Kent, D. C., Park, R. (1971). Flexural members with confined concrete. *Journal of Structural Engineering*, **97:7**, 1969−1990.

Mazzoni, S. , McKenna, F. , Scott M.H. , Fenves G. L., et al. (2005). OpenSees user manual for Opensees version 1.7.3., University of California, Berkeley.

McKenna, F., Fenves, G. L., and Scott, M. H. et al. (2006). OpenSees: Open system for earthquake engineering simulation., http://opensees.berkeley.edu. University of California, Berkeley.

Panagiotakos, T.B., Bardakis, V., Fardis, M.N. (2006) Displacement-based Seismic Design Procedure for Concrete Bridges with Monolithic Connection between Deck and Piers Proc. Proceedings of 2nd fib Congress, Napoli.

Priestley, M.J.N., Calvi, G.M., and Kowalsky, M.J. (2007). *Displacement-Based Seismic Design of Structures*, IUSS Press, Pavia, Italy.

Priestley, M. J. N. and Grant, D. N., (2005). Viscous Damping in Seismic Design and Analysis. *Journal of Earthquake Engineering*, **9:Special issue 2**, 309-330.

Restrepo J.C.O. (2007). *Displacement-based design of continuous concrete bridges under transverse seismic excitation*. Master Thesis, Rose School, Pavia.

Scott, M.H. and Fenves, G. L. (2006). Plastic Hinge Integration Methods for Force-Based Beam-Column Elements, *Journal of Structural Engineering*, **132:2**, 244-252.

Vamvatsikos, D. and Cornell, C.A. (2002). Incremental dynamic analysis. *Earthquake Engineering and Structural Dynamics,* **31:3**, 491-514.